JOURNAL OF MATERIALS SCIENCE **28** (1993) 40–44

Preparation and thermoelectricity of TiO_2/V_2O_5 powders

F. ANSORGE, C. RÜSSEL
Institut für Werkstoffwissenschaften III (Glas und Keramik), Universität Erlangen-Nürnberg, 8520 Erlangen, Martensstrasse 5, Germany

TiO_2/V_2O_5 powders were prepared by the mixed oxide and sol–gel method. The sols were dried using different procedures. The obtained powders were characterized by X-ray diffraction, scanning electron microscopy, BET-adsorption and laser granulometry. The electric properties were determined by measuring the thermoelectric power. A strict correlation of the thermoelectric power and the V_2O_5 content could be observed, but by contrast to conductivity measurements, the thermoelectric power was not influenced by the powder morphology. Additionally, the thermoelectric power was drastically influenced by the calcination temperature.

1. Introduction

TiO_2/V_2O_5 catalysts are widely used to remove NO_X from waste gases [1] and for the selective reduction or oxidation in organic chemistry, e.g. the oxidation of *o*-xylene to phthalic acid [2], or the preparation of niconitrile [3]. The dependence of catalytical properties on the electric, e.g. semiconducting, behaviour has often been discussed theoretically (e.g. [4–6]). On the other hand, the electrical properties of powders are strongly influenced by the preparation procedure. If the electrical conductivity of (previously compacted, e.g. cold pressed) powders is measured, the values are strongly affected by the measuring techniques, e.g. the method of compaction, and can only provide reliable qualitative data, if the morphology of the powders investigated is similar. Therefore, the electrical conductivity of powders can scarcely be related to intrinsic properties, if powders are prepared by very different procedures and consequently possess very different morphology. Measurements of the thermoelectricity, however, should provide information which is not influenced by the morphology and the conditions of the compaction process. This paper deals with the influence of the preparation method on the powder morphology and the thermoelectric properties.

2. Experimental procedure

2.1. Preparation of TiO_2/V_2O_5 powders

TiO_2/V_2O_5 powders were either prepared by the mixed oxide or a sol–gel method. Using the mixed oxide method, TiO_2 (Degussa P 25) and different quantities of ammonium metavanadate were mixed in ethanol and subsequently, the solvent was evaporated at 80 °C and calcined at 900 °C hereby ammonium metavanadate was thermally decomposed to V_2O_5 and ammonia. Sol–gel powders were prepared by using titanium ethoxide (Ventron), ethanol (Merck), water and nitric acid (Merck) in molar ratios of 1 : 1 : 2 : 0.4 and various concentrations of $VOCl_3$ (Ventron). The $VOCl_3$ addition was carried out during cooling very slowly to avoid drastic heating of the solution due to the strongly exothermic reaction of $VOCl_3$ with water.

The obtained solution was dried using four different procedures: it was dropped into petrol-ether and subsequently filtrated (A) or into paraffin (B) and subsequently heated to 80 °C under heavy stirring. In another series of experiments, the sol was dropped into hot paraffin (C) which was previously heated to 150 °C. As a fourth method (D), the solution was dried in a minispray dryer (Büchi 190) using a spray flow of 230 °C. All four types of powder were subsequently calcined at temperatures of 550 or 900 °C.

2.2. Characterization

The powders obtained were characterized by X-ray diffraction (XRD, Siemens Diffrac 500), scanning electron microscopy (SEM, Cambridge Instruments), electron paramagnetic resonance (EPMR, Bruker ER 414), BET adsorption (Micromeritics ORR 2100D) and laser granulometry (Cilas 715).

The thermoelectric power was measured using a self-constructed apparatus schematically shown in Fig. 1. The powder was slightly compacted to increase the electrical conductivity. The thermoelectric power was measured with the aid of an electrometer (Keithley electrometer 610 B) as a function of the temperatures T_1 and T_2.

3. Results and discussion

Table I summarizes the mean grain sizes and specific surface areas of the different powders. It can be seen

0022–2461 © *1993 Chapman & Hall*

TABLE I Mean grain size and specific surface area of the obtained powders

Preparation method	Calcination temperature (°C)	Mean grain size (µm)	Specific surface area ($m^2 g^{-1}$)
A Petrol-ether	550	6.7	2.7
B Paraffin drying	550	37.3	53
C Hot paraffin drying	550	13.5	29
D Spray drying	550	3.75	5.1
	900	5.33	1.5

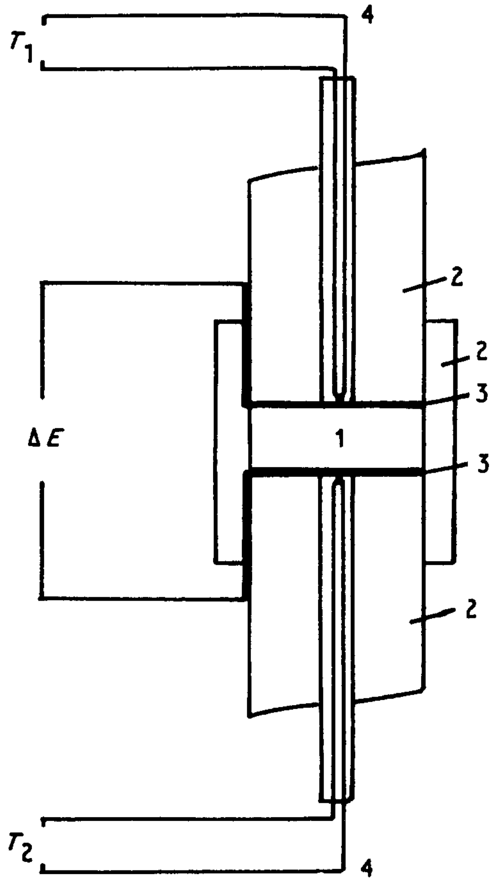

Figure 1 Schematical drawing of the apparatus used for thermoelectricity measurements. 1, powder sample; 2, alumina tubes; 3, platinum electrodes; 4, thermocouples.

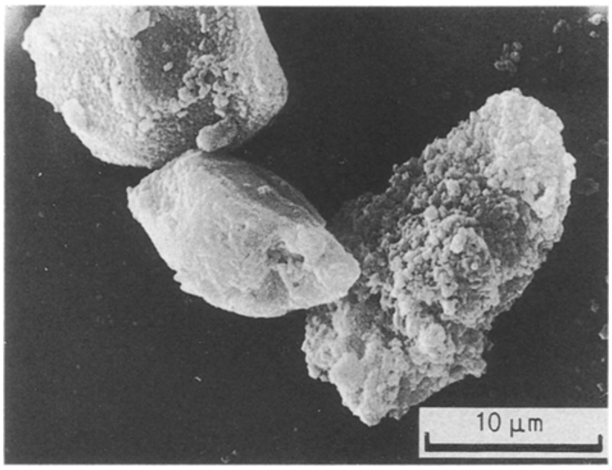

Figure 2 Scanning electron micrograph of hot paraffin-dried powder calcined at 550°C.

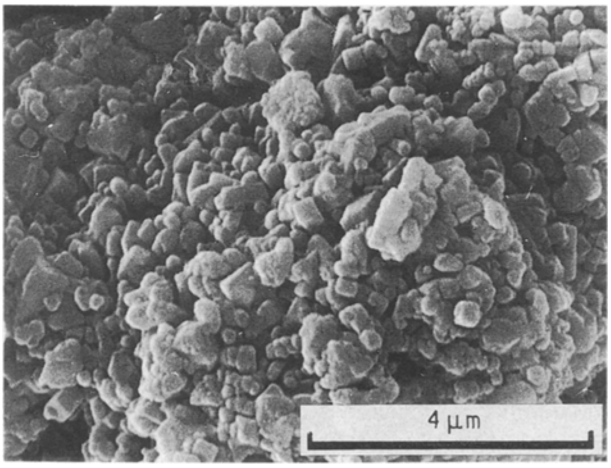

Figure 3 Scanning electron micrograph of hot paraffin-dried powder calcined at 550°C. (higher magnification)

that the specific surface areas did not increase with decreasing mean grain size. For example, the paraffin-dried powder (B) possessed both the largest mean grain size and the highest specific surface area. Figs 2–5 show scanning electron micrographs of powders prepared by different procedures. In Fig. 2, hot paraffin-dried powder (C) can be seen. The grains were fairly coarse; nevertheless, as shown in Fig. 3, the particles themselves were very porous. In Fig. 4, spray-dried powder can be seen; the particles were mainly spherical or hollow spherical as is typical for spray-dried powders. The surface was very smooth and there was no evidence of any internal porosity of the particles. By contrast, spray-dried powder calcined at 900°C possessed very different morphology and a larger mean grain size, as can be seen in Fig. 5.

Fig. 6 shows EPMR spectra of spray-dried powders, calcined at 550 and 900 °C. The spectrum of the sample calcined at 900 °C exhibited only one peak without hyperfine splitting, while the other spectrum showed various peaks and strong hyperfine splitting. ^{47}Ti (natural abundance 7.28%, spin 5/2) and ^{49}Ti (natural abundance 5.51%, spin 7/2) are the only nuclei of titanium possessing a nuclear spin [7] and hence hyperfine splitting. By contrast, vanadium predominantly consists of ^{51}V (natural abundance 99.76%) with a nuclear spin of 7/2 [7] and therefore shows hyperfine splitting. Although both spectra are superpositions of the Ti^{3+} and V^{4+} spectra, it can be concluded that the paramagnetism of the samples calcined at 550 and 900°C was predominantly due to the occurrence of V^{4+} and Ti^{3+}, respectively. It

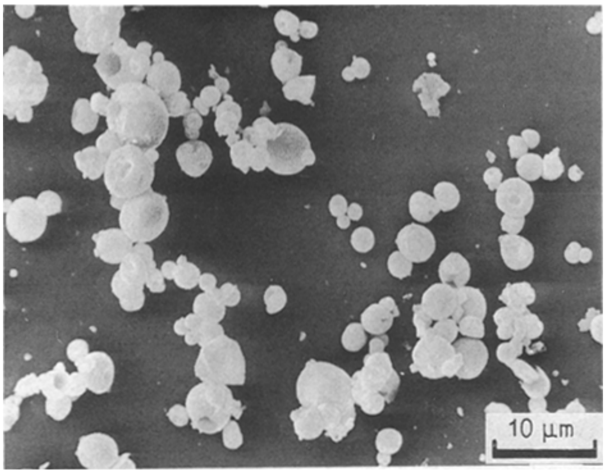

Figure 4 Scanning electron micrograph of spray-dried powder calcined at 550°C.

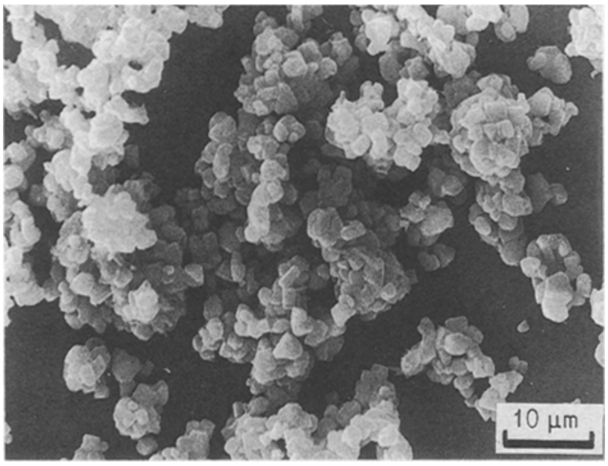

Figure 5 Scanning electron micrograph of spray-dried powder calcined at 900°C.

should be noted that other materials, e.g. glass doped with V^{4+} or Ti^{3+}, show very similar spectra [8].

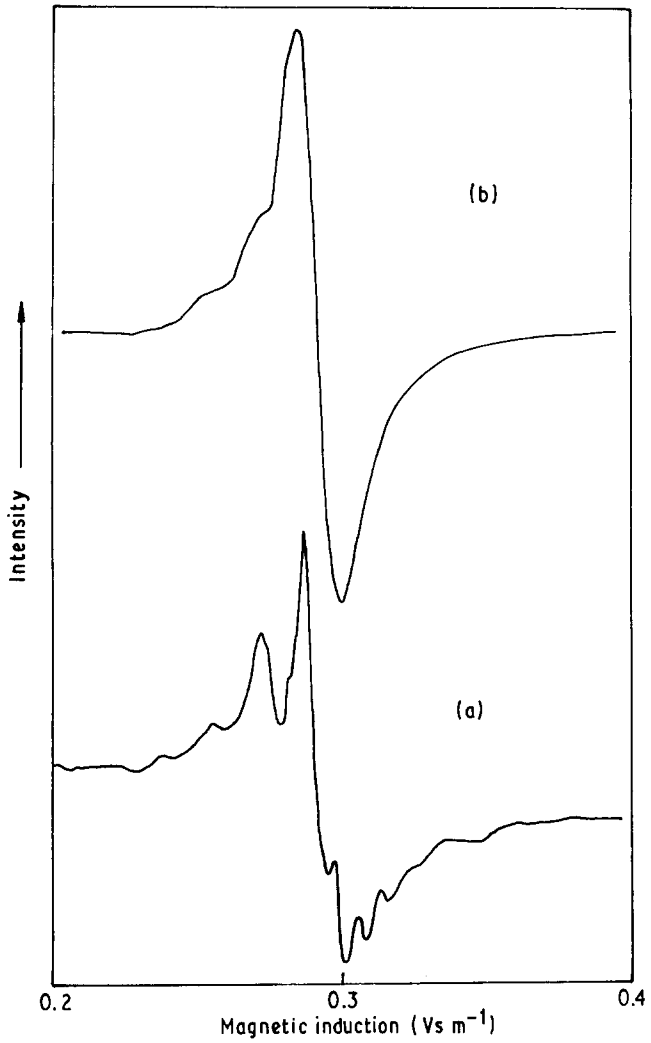

Figure 6 EPMR spectra of spray-dried powders calcined at (a) 550 and (b) 900°C.

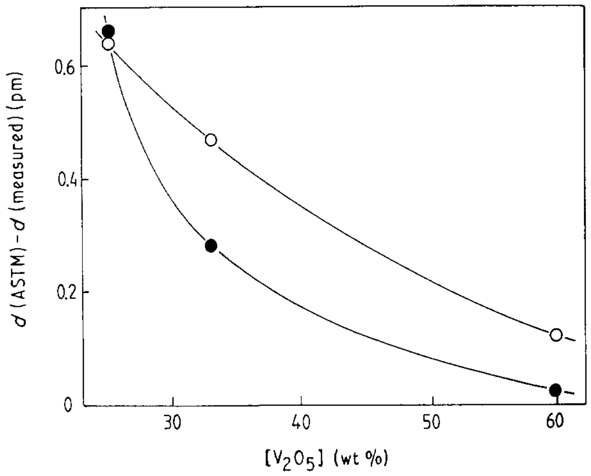

Figure 7 Dismatch of the V_2O_5 [4 0 0] and V_2O_5 [3 1 0] peak in the XRD patterns to the *d*-values of the ASTM card. (●) Rutile, (o) anatase.

XRD patterns of powders calcined at 900°C matched those of rutile [9] and V_2O_5, depending on the quantity of vanadium doping [10]. Powders prepared by the addition of 5 and 10 wt% V_2O_5 showed only lines related to TiO_2, while those containing at least 12.5 wt% V_2O_5 exhibited additional lines. By contrast, XRD patterns of samples calcined at 550°C matched that of anatase [11]. For V_2O_5 concentrations up to 8 wt%, additional peaks could not be observed, while those samples containing higher quantities of V_2O_5 showed these lines. These additional lines approximately matched those of V_2O_5, but there were notable deviations in the 2Θ values depending on the amount of vanadium added. In Fig. 7, these deviations are illustrated as the *d*-values obtained from the ASTM card 9-387 and the two intensive V_2O_5 peaks ([4 0 0] and [3 1 0]). This mismatch decreased with increasing quantity of V_2O_5 and was zero for 50 and 70 wt% V_2O_5 for rutile and anatase, respectively. It should be assumed that V_2O_5 crystallizes with its [0 1 0] plane on to the [0 1 0] plane of anatase [12] or the [0 1 0] plane of rutile [13]. On to all other planes of rutile and anatase, V_2O_5 will crystallize semi- or noncoherently in the first layer. This results in a distortion of the V_2O_5 lattice which causes a mismatch in the XRD patterns. For increasing vanadium concentrations, V_2O_5 will grow more and more from the non-coherent layer in the undistorted V_2O_5 lattice.

In Fig. 8, thermoelectric potentials of TiO_2/V_2O_5 (mixed oxide method, calcined at 900°C) with the addition of 5 and 15 wt% V_2O_5 are shown. They were measured as a function of the temperature difference ($T_1 - T_2$, see Fig. 1, T_1 was approximately room temperature or slightly above). A fairly good correlation between the measured potential and the temperature difference was obtained enabling calculation of standard Seebeck coefficients as defined by Equation 1.

$$\alpha = \frac{\mathrm{d}E}{\mathrm{d}T} \tag{1}$$

In the temperature range shown in Fig. 8, the standard Seebeck coefficients were nearly independent of temperature and possessed lower values if the quantity of V_2O_5 was increased. By contrast, a drastic dependence of the standard Seebeck coefficient on the temperature and the amount of V_2O_5 was observed in sol–gel derived anatase powders calcined at 550°C (see Fig. 9). At higher temperatures, the standard Seebeck coefficients were nearly constant and had values in the range -0.4 to -0.6 mV K^{-1}. By lowering the temperature, however, a drastic decrease could be observed and within a range 20–50°C, values of -1.5 mV K^{-1} and lower were reached. In all anatase samples investigated, this drastic decrease occurred; the corresponding temperatures, however, were fairly different and lay within the range 300–470 K.

This behaviour can be described by several approaches. Firstly, the well-known "transition" caused by a magnetic exchange interaction of the 3d electrons. Most vanadium oxides show this behaviour with increasing temperature reaching from semiconductivity to metallic conductivity. Secondly, the phenomenon can be described by a Mott transition for which only a small energy gap is required. Fig. 10 shows a drawing of the onset temperature, T_o (at a constant arbitrary value of $\alpha = -1.5$ mV K^{-1}) against the V_2O_5 content. A linear correlation can be observed.

Fig. 11 shows standard Seebeck coefficients of TiO_2/V_2O_5 powders with very different quantities of V_2O_5. Some powders were prepared using the sol–gel route, calcined at 550°C and therefore possessed an

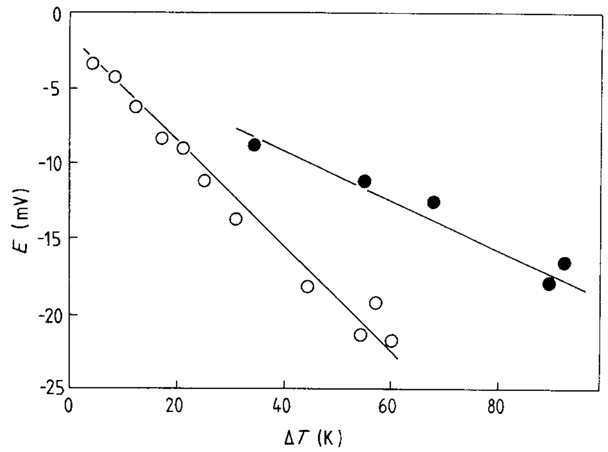

Figure 8 Thermoelectric power measured at powders prepared by the mixed oxide method at various temperatures differences (calcined at 900°C).
(●) 5 wt% V_2O_5, (○) 15 wt% V_2O_5

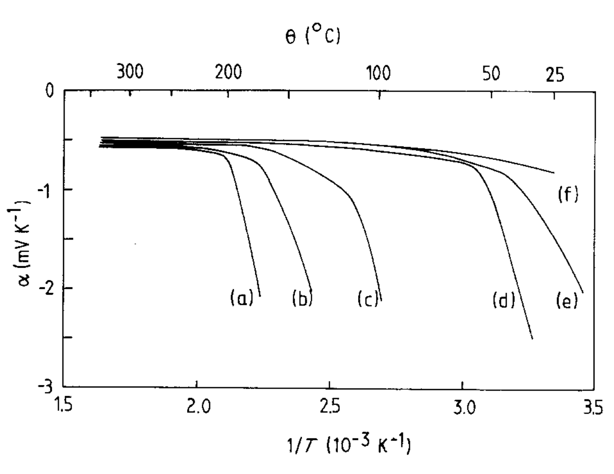

Figure 9 Standard Seebeck coefficients of spray-dried powders for various temperatures and quantities of V_2O_5 doping (calcined at 550°C). (a) 8 wt%, (b) 24 wt%, (c) 38 wt%, (d) 50 wt%, (e) 60 wt%, (f) 100 wt%.

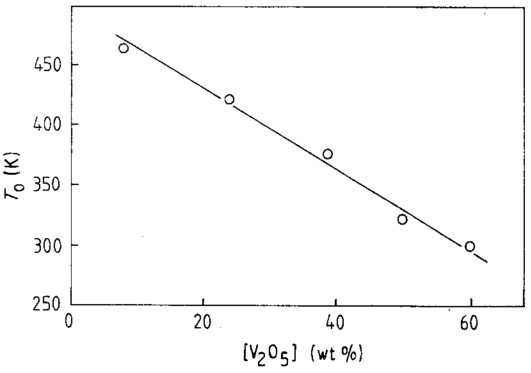

Figure 10 Onset temperature (at $\alpha = -1.5$ mV K^{-1}) as a function of the V_2O_5 content. (anatase powders calcined at 550°C)

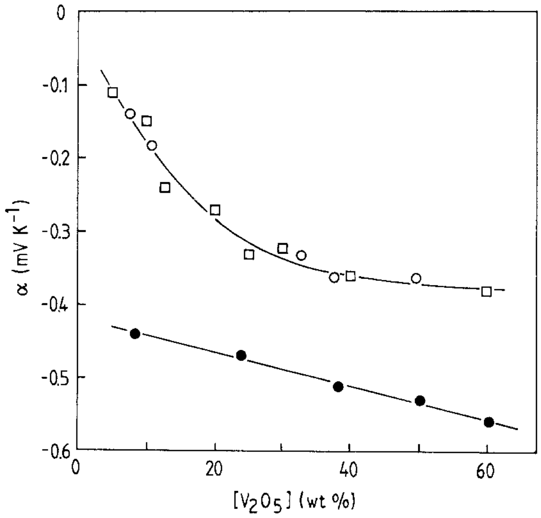

Figure 11 Standard Seebeck coefficients of powders doped with various quantities of V_2O_5. (□) Mixed oxide powder calcined at 900°C (rutile), (○) spray-dried powder calcined at 900°C (rutile), (●) spray-dried powder calcined at 550°C (anatase).

anatase lattice (see dots in Fig. 11). These values have been measured at comparably high temperatures at which they are constant. Other samples were prepared by either using the mixed oxide method (see squares in Fig. 11) or by the sol–gel route (see circles in Fig. 11). These samples were calcined at 900°C and possessed a rutile lattice. The standard Seebeck coefficient of powders with a rutile lattice decreased with increasing quantity of V_2O_5 and reached a nearly constant value of -0.37 mV K^{-1} at V_2O_5 concentrations of more than 30 wt%. These values apparently did not depend on the kind of preparation method (sol–gel or mixed oxide), although the morphology of these powders was different. This is a very notable result because it proves well that, in contrast to measurements of the electrical conductivity, measurements of the thermoelectricity are not influenced by the powder morphology.

The calcination temperature, however, strongly influenced the standard Seebeck coefficients. For samples calcined at 550°C, the influence of the quantity of V_2O_5 was much lower. The standard Seebeck coefficients possessed much lower values, e.g. -0.44 mV K^{-1}, in comparison with -0.13 mV K^{-1} for a rutile powder with the same V_2O_5-concentration (8 wt%) and the influence of the quantity of V_2O_5 was not as large.

4. Conclusions

Using both mixed oxide and sol–gel methods, a large variety of powder morphologies can be obtained. Powders possessing large mean grain size and large BET surfaces, as well as powders possessing small mean grain sizes and small BET surfaces, can be obtained. The standard Seebeck coefficients strongly depend on the quantity of V_2O_5 added, on the calcination temperature, and the temperature at which they are measured, but they are independent of the powder morphology. Therefore, the measurement of the thermoelectricity is assumed to be a suitable method for investigating the semiconducting properties of powders and hence the catalytic properties.

References

1. E. RICHTER, K. KNOBLAUCH and H. JÜNGTEN, *Chem. Ing. Tech.* **52** (1980) 456.
2. F. WIRTH, in "Ullmanns Enzyklopädie der Technischen Chemie," Vol. 18 (Verlag Chemie, Weinheim, 1979) p. 521.
3. A. ANDERSON and S. T. LUNDINI, *J. Catal.* **58** (1980) 383.
4. K. HAUFFE and TH. WOLKENSTEIN (eds), "Symposia on electronic phenomena in chemisorption and catalysis," (de Gruyter, Berlin, 1969).
5. TH. WOLKENSTEIN, "Elektronentheorie der Katalyse an Halbleitern," (VEB Verlag der Wissenschaften, Berlin, 1964).
6. J. J. JOFFE and L. M. PISSMEN, "Heterogene Katalyse" (Akademie Verlag, Berlin, 1975).
7. BRUKER ALMANACH, Bruker Institute, Bruxelles, Belgium (1986).
8. B. CAMARA, *Ber. Dt. Keram. Ges.* **56** (1979) 25.
9. ASTM card 21-1276.
10. ASTM card 9-387.
11. ASTM card 21-1272.
12. A. VEJUX and P. COURTINE, *J. Sol. State. Chem.* **23** (1978) 1009.
13. M. INOMATA, A. MIYAMOTO and M. MURAKAMI, *JCS Chem. Comm.* (1988) 233.

Received 2 August 1991
and accepted 7 May 1992